

A SYSTEMATIC INVESTIGATION OF STRAIN RELAXATION, SURFACE MORPHOLOGY AND DEFECTS IN TENSILE AND COMPRESSIVE InGaAs/InP LAYERS

C. FERRARI*, L. LAZZARINI*, G. SALVIATI*, M. NATALI°, M. BERTI°, D. DE SALVADOR°, A.V. DRIGO°, G. ROSSETTO^, G. TORZO^

*CNR-MASPEC Institute, Parco Area delle Scienze 37/A, I-43010 Fontanini- Parma, Italy

° INFN, Department of Physics, University of Padova, Via Marzolo 8, I-35131 Padova, Italy

^ CNR-ICTIMA Institute, Corso Stati Uniti 4, I-35127 Padova, Italy

ABSTRACT

The results of a systematic investigation by transmission electron microscopy (TEM), cathodoluminescence (CL), Rutherford backscattering (RBS), X-ray diffraction and topography and scanning force microscopy (SFM) techniques on several InGaAs/InP compressive and tensile strained layers covering the misfit range from -2.3 to 1.5×10^{-2} and grown by the metal organic vapor phase epitaxy (MOVPE) technique are reported. In compressively strained films the same dependence for the residual strain vs the film thickness as for the InGaAs/GaAs is found whereas a different strain release rate and different extended defects are found in tensile stressed InGaAs alloy. In particular in tensile stressed samples, grooves, planar defects and cracks are present in addition to the interfacial network of misfit dislocations. The correlation between the observed planar defects and the mechanisms of strain relaxation in the case of tensile strained layers is discussed.

INTRODUCTION

The strain relaxation mechanism for lattice mismatched epitaxial layers under compressive strain has been extensively studied, in particular for the InGaAs/GaAs system (Drigo et al 1989 [1], Lavoie et al. 1995 [2]). For layers under tensile strain such as InAlSb/InSb it has recently been suggested (Maigné et al. [3]) that the relaxation mechanism might be different since the residual strain is significantly larger than in InGaAs/GaAs layers with comparable misfit. However a quantitative comparison between the two systems is not necessarily appropriate because the materials exhibit different physico-chemical, mechanical and thermal properties.

The $\text{In}_x\text{Ga}_{1-x}\text{As}/\text{InP}$ material system is ideal for the direct comparison of the relaxation processes involved in compressive and tensile strains. In fact, varying the In composition below or above $x=0.53$, the epitaxial layer shows negative or positive lattice mismatch.

EXPERIMENT

Thirty-seven InGaAs epitaxial films were grown on (001) semi-insulating InP substrates via metalorganic vapor phase epitaxy (MOVPE) in order to cover large intervals of Indium concentration (0.2 to 0.73) and film thickness (8 to 2400 nm).

TEM bright-field and dark-field images of $\langle 001 \rangle$ plan view and $\langle 110 \rangle$ cross-sections were recorded with a JEOL 2000 FX microscope at 200 kV on mechanically and chemically thinned samples finished by argon ion-milling (Gatan 600 Duo Mill).

The indium composition and strain of the layers were determined by high-resolution X-ray diffraction (Philips MRD) measuring rocking curves of symmetric (004) and asymmetric (444) reflections along the $\langle 110 \rangle$ in-plane directions both in grazing incidence and grazing emergence geometry. X-ray topographs were recorded by using a conventional Lang camera using the 115 asymmetric diffraction condition and the $\text{CuK}\alpha$ wavelength. RBS measurements were

performed with 2MeV 4He⁺ beams at the Van de Graaf accelerator (LNL Legnaro) to determine the layer thickness and to cross-check the indium compositions.

The surface morphology was investigated by a scanning force Park CP microscope operated in contact-mode, using ultra-lever™ tips with nominally 10 nm tip radius.

RESULTS

Strain Release in InGaAs/InP Layers

In the compressive case (In concentration in the interval $0.61 < x < 0.73$) the strain relaxation along the two 110 directions is nearly symmetric. The residual strain as a function of the layer thickness follows the empirical curve previously found for MBE grown InGaAs/GaAs layers with In concentration < 0.2 [1]. The main result is that strain relaxation in compressive InGaAs layers is independent of both growth conditions and Indium composition [4].

Tensile strained InGaAs layers (In concentration varying in the interval $0.2 < x < 0.36$) exhibit a relevant asymmetry in the strain release between [110] and [1-10] directions, the strain along the [110] direction relaxing at a layer thickness lower than for the [1-10] direction (Lazzarini et al. [5]). Such a difference increases if the misfit is decreased. Fig. 1) reports the average residual strain of InGaAs/InP tensile layers in a In composition range between 0.35 and 0.2. It is evident that the onset of strain release, which appears at the points where the strain-thickness curves change slope, is shifted toward higher layer thickness values with respect to compressive layers. Once initiated, however, the strain relaxation proceeds much faster than for compressive layers. It is evident from the figure that it is not possible to fit the experimental curves with a single curve. As shown later the types of extended defects in tensile layers are very different from compressively strained ones. This suggests that extended defects are responsible for the retarded strain release.

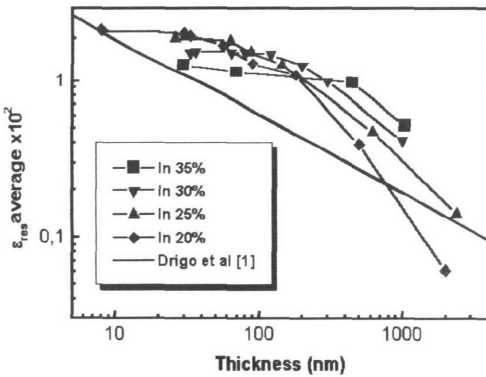


Fig. 1: average residual strain along [110] and [1-10] of InGaAs/InP tensile layers

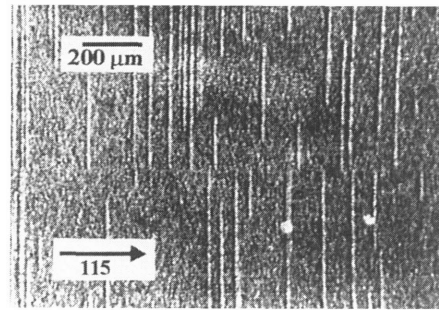


Fig. 2 : CuKα (115) reflection topograph of a 0.2 μm thick InGaAs/InP layer close to the lattice match.

Extended Defects Characterization

In compressive InGaAs/InP relaxed layers the only extended defects present are misfit dislocations (MD), 60° mixed in character, arranged in the usual orthogonal network at the interface between the epilayer and the substrate and whose density accounts for the measured

relaxation. Surface morphology is affected by the typical cross-hatch pattern observed in relaxed heterolayers.

Fig. 2 reports a detail of a X-ray topography of a tensile InGaAs/InP layer close to the lattice match showing single misfit dislocation segments a few mm long which end in correspondence of an extended defect line. The very faint contrast of the line excludes this as a simple 60° misfit dislocation line since the product $b \cdot h$ would not be zero, as required by the contrast extinction rule. In comparison with compressively strained InGaAs/GaAs layers which exhibit much longer MD lengths (Ferrari et al.[6]), the topograph of fig. 2 demonstrates the effective interaction between structural defects in tensile strained layers during the strain release process.

The analysis of the surface morphology has been performed by scanning force microscopy. For tensile strained layers one of the main morphology differences with respect to compressive samples is the development of V-shaped grooves along [1-10] and [110], which appears in correspondence with the onset of measurable strain relaxation along the respective perpendicular directions. Grooves appear at the beginning of strain release along the [1-10] direction and only a lower density of broad [110] oriented grooves appear. While grooves deepen and widen as the layer thickness increases, their density does not change significantly. On the contrary, fig. 3 shows the rapid increase of groove density with the layer misfit.

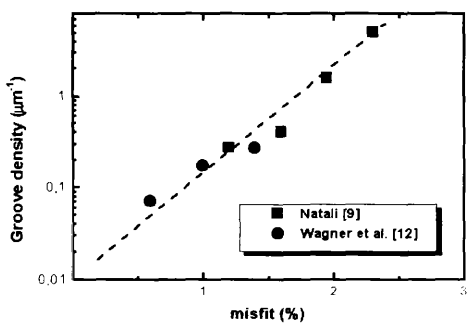


Fig. 3: groove density vs layer misfit along [110] direction

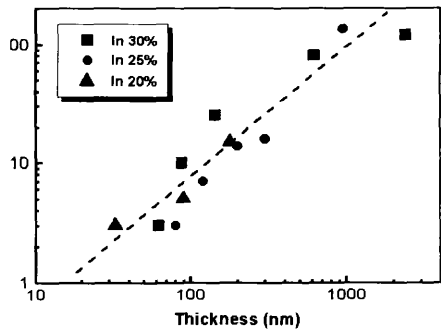


Fig. 4: average groove depth vs thickness along [110] direction measured by SFM for different composition values

The average groove depth as a function of layer thickness along the [110] direction and for different composition values is shown in fig. 4. These data show that no matter the degree of strain release the average groove depth is approximately 10% of the layer thickness. Nevertheless a smaller groove density with depths of the same order of the layer thickness are evidenced by SFM observations and TEM micrographs along the [1-10] direction (fig 5). The groove side-walls often coincide with the {111} planes but faceting occurs also on higher index {11h} planes. Okada et al. [7] demonstrate that the appearance of surface faceting in MBE grown InGaAs/InP tensile strained layers can be explained in term of the reduction of elastic energy in the layer.

Figure 6 shows a plan-view TEM image of a network of strongly interacting stacking faults and/or twins which reproduces the groove in-plane arrangement as it is observed by SFM. We thus believe that stacking fault of twins are correlated to the formation of grooves and coexist with a network of misfit dislocations contributing to the strain release. In fact only in low misfit samples where the groove density is low, the density of misfit dislocation accounts for the amount of relaxed misfit measured by XRD.

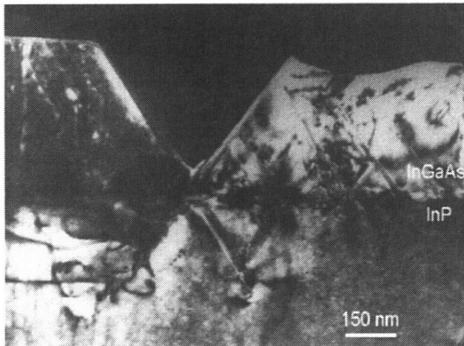


Fig. 5: TEM image of a groove running along [1-10] direction with depth equivalent to the layer thickness

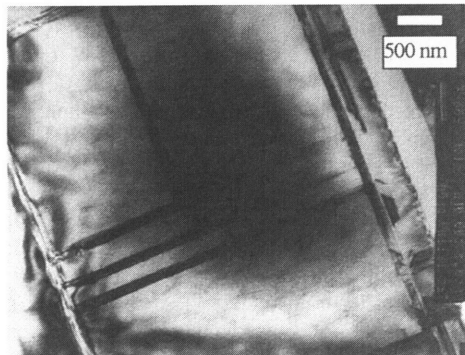


Fig. 6: [110] zone axis plan-view TEM image showing stacking faults and/or twins

DISCUSSION AND CONCLUSIONS

Layers under compression present the same defects and morphology and relax following the same thickness dependence as that found for MBE grown InGaAs/GaAs showing no composition or growth technique effect. Since the larger Indium composition and the higher growth temperature of the present samples significantly increase the dislocation glide velocity [8] it is possible to conclude that the strain release rate cannot be due to kinetic limitation to the dislocation glide.

In the tensile InGaAs/InP relaxed layers, in addition to the interfacial misfit dislocation network, V-shaped grooves are present. In cross section TEM observations stacking faults and twins were observed in the groove bottom part. From the observation that misfit dislocations and grooves appear first along the [1-10] direction parallel to the first MDs we can deduce that the grooves must have a relevant role in the strain relaxation mechanism. Two possible mechanisms are suggested to evaluate such a contribution:

- a) the presence of a surface faceting or grooves can reduce the total energy of the system by elastic strain release with a decrease of the local strain value
- b) grooves reduce the local film thickness and act as a barrier for the glide of misfit dislocation threading segments running in the orthogonal direction.

Okada et al. [6]) calculated the decrease of the elastic energy ΔE of a faceted surface of depth $2h$ and spacing λ , in the case of $h \ll \lambda$. Even if we found the depth h to be almost equivalent to the groove dimension λ , from the expression of the elastic energy in a uniformly deformed film given by Matthews et al. [10] we can evaluate the elastic energy reduction $\Delta E/E$ due to the surface morphology:

$$\frac{\Delta E}{E} \approx \frac{\pi(1-\nu)^2}{4(1+\nu)} \cdot \frac{h^2}{\lambda t} \quad (1)$$

where ν is the Poisson ratio.

Assuming the value $h/t \approx 0.1$ determined in our samples (Natali [9]), the reduction of the strain energy depends on h/λ so that the average strain, proportional to the square root of the elastic energy, is reduced by

$$\frac{\Delta\epsilon}{\epsilon} \approx 0.2 \cdot \sqrt{\frac{h}{\lambda}} \quad (2)$$

due to the surface morphology. Equation 2 partially accounts for the observed discrepancy between strain release and misfit dislocation density measured by TEM in samples with larger misfit value. Nevertheless in our samples groove depths comparable to the width were observed, so that a larger contribution to the strain reduction near the grooves is expected.

According to the model of Matthews et al. [10] the local reduction of the layer thickness due to the groove decreases the driving force for the movement of threading dislocation segments during the strain release. This effect is equivalent to the blocking due to dislocation pile-up suggested by Fitzgerald et al. [11] and explains the delay in the strain release along the [1-10] direction. Furthermore V-shaped grooves are often accompanied by the presence of stacking fault that can act as a barrier for misfit dislocation propagation.

Therefore for a given misfit value the onset of strain release would occur at thickness values larger than for compressive strained film. Also the increase of groove density as a function of layer misfit as found by Wagner et al. [12] and Natali [9] is in qualitative agreement with the increase of the blocking effect in the perpendicular direction in layers with larger misfit.

In addition to grooves and stacking faults, in tensile strained samples a significant density of cracks has also been found. Nevertheless, simple calculations show that in our samples the maximum amount of misfit relaxed by cracks turns out to be a negligible quantity and close to the amount of tensile thermal strain added to the layer during the post-growth cool-down ([4], [5]). Such finding and the evidence of crack formation after the cooling indicate that crack formation cannot have any influence in the strain release mechanism.

REFERENCES

1. A.V. Drigo, A. Aydinli, A. Carnera, F. Genova, C. Rigo, C. Ferrari, P. Franzosi and G. Salviati, *J. Appl. Phys.* **66**, p. 3334 (1989)
2. C. Lavoie, *Appl. Phys. Lett.* **67** (25), p. 3744 (1995)
3. P. Maigné, D.J. Lockwood, C. Dharma-Vardana, J.B. Webb, *J. Appl. Phys.* **77**, 1466 (1995)
4. A.V. Drigo, M. Natali, M. Berti, D. De Salvador, G. Rossetto, G. Torzo, G. Carta, L. Lazzarini, G. Salviati in *Lattice Mismatch and Heterovalent Thin Film Epitaxy*, edited by E. Fitzgerald, TMS proc. 1999
5. L. Lazzarini, *proc. of Microscopy of Semiconducting Materials XI*, In press 1999
6. C. Ferrari, S. Gennari, G. Salviati, M. Natali, A.V. Drigo, G. Rossetto, M. Currie, E.A. Fitzgerald in *Lattice Mismatch and Heterovalent Thin Film Epitaxy*, edited by E. Fitzgerald, TMS proc. 1999
7. T. Okada, G.C. Weatherly, D.W. McComb, *J. Appl. Phys.* **81**, p. 2185 (1997)
8. K. Sumino and I. Yonegana, *proceedings of 7th Semi-insulating III-V materials Conference* ed C.J. Miner, W. Ford, and E.R. Weber (Bristol, Institute of Physics 1992), **29**
9. M. Natali in *Strain relaxation, defect formation and surface morphology in tensile and compressive InGaAs/InP layers*, PhD Thesis, University of Padova (1998)
10. J. W. Matthews and A.E. Blakeslee, *J. Cryst. Growth* **27**, p. 118 (1974)
11. E.A. Fitzgerald, S.B. Samavedam, Y.H. Xie, L.M. Giovane, *J. Vac. Sci. Tech. A* **15**, p. 1048 (1997)
12. G. Wagner, V. Gottshalk, R. Franzheld, S. Kriegel, P. Paufler, *Phys. Stat. Sol. (a)* **146**, p. 371 (1994)